Preparation of mesoporous catalyst supported on silica with finely dispersed Ni particles

Young Sung Cho, Jong Chul Park, Byunghwan Lee, Younghun Kim, and Jongheop Yi *
School of Chemical Engineering, Seoul National University, San 56-1 Shillim, Kwanak, Seoul 151-742, Korea

Received 19 May 2001; accepted 10 January 2002

A novel nickel catalyst supported on SBA-15 type mesoporous silica was synthesized by the grafting of N-(trimethoxysilylpropyl)ethylene diamine triacetic acid salt (EDTA) onto the surface of SBA-15 and followed by adsorption of nickel ions and calcinations (Ni-E-SBA). The catalysts prepared were characterized using XRD, TEM, TED, SAXS and N_2 adsorption/desorption measurements. While nickel particles loaded on catalysts prepared by the wet impregnation method were found to be aggregated on the outer wall of the supports, nickel particles were finely dispersed on the surface of the mesopores in the Ni-E-SBA catalyst. The catalytic performances of the prepared catalysts were evaluated using the hydrodechlorination (HDC) of 1,1,2-trichloroethane (TCEa) as a model reaction. Results showed that the Ni-E-SBA catalyst had the highest activities of the catalysts examined under the given conditions.

KEY WORDS: Ni loaded SBA-15; EDTA grafting; hydrodechlorination; trichloroethane.

1. Introduction

Since the introduction of MCM-41 and FSM, a variety of mesoporous molecular sieves, such as HMS, SBA-15 and KIT-1, have been developed [1–5]. Because of their desirable properties as a catalyst support, *e.g.*, large surface area, controllable pore size and narrow pore-size distributions, these types of materials have attracted considerable attention for catalyst preparation [6–10]. However, investigations focused on the metal-loading procedures, in order to properly use the superior properties, have been minimal. Direct synthesis [6,8], impregnation [8,9] and ion-exchange [10] methods have been used to load metals on the mesoporous molecular sieves for the preparation of catalysts to date. However, some limitations are anticipated in these methods, such as low metal-loading capacity (ion exchange), pore blockage by metal particles (impregnation) and weak pore structure (direct synthesis). As a result, there is a need to develop a novel metal-loading method to utilize the advantages of the mesoporous molecular sieve as a catalyst support.

It is widely recognized that metal-chelating agent functionalized silica can adsorb metal ions, and a number of studies have been reported on this issue [11–14]. Feng *et al.* [11] synthesized thiol-monolayered mesoporous molecular sieves for the adsorption of mercury ions in aqueous solutions. Diaz *et al.* [12] synthesized ethylenediamine, diethylenetriamine and ethylenediaminetriacetic acid salt functionalized mesoporous silicas by grafting method. Cobalt complexes were bound on these functionalized mesoporous silicas. Similar studies [13,14] have been performed for the treatment of wastewater containing various kinds of heavy metals. In this work, a nickel-loaded catalyst was synthesized using a metal-chelating agent functionalized mesoporous molecular sieve. Functional groups were grafted on the surface of as-synthesized mesoporous silica, followed by the adsorption of nickel ions and calcinations. This work is the first attempt to apply these methods for the synthesis of mesoporous catalysts. The catalyst prepared is expected to have ordered pore structure, moderate metal-loading capacity and fine dispersion of metal on the mesopores.

In this work, we chose hydrodechlorination (HDC) of trichloroethane (TCEa) as a model system for the test of nickel catalysts. Catalytic hydrodechlorination is recognized as a promising recycling process for the treatment of chlorinated hydrocarbons, which are produced as a waste or by-products. However, no attempts have been made to find a general procedure for this process. Among the various approaches, nickel-loaded catalysts are the most obvious for use in catalytic hydrodechlorination [15–17]. TCEa was chosen as a model compound, since it was one of the major by-products in the ethylene dichloride production process. The catalytic performance of prepared catalysts was compared and properties of each catalyst were investigated using XRD, TEM, TED, SAXS and N_2 adsorption/desorption measurements.

2. Experimental

2.1. Catalyst preparation

SBA-15 mesoporous silica was synthesized using a non-ionic surfactant, Pluronic P123 (poly(alkylene) oxide triblock copolymer, BASF Co.), as a template

* To whom correspondence should be addressed.

1011-372X/02/0700-0089/0

and tetraethylorthosilicate (TEOS, Aldrich Chemical Co.) as a silica precursor [4]. N-(trimethoxysilylpropyl)ethylene diamine triacetic acid salt (EDTA, Gelest Inc.) was used as a metal-chelating agent. The acidic solution of surfactant and silica precursor was stirred at 313 K for 20 h and aged at 353 K for 24 h. The solid product was filtered and template was removed by ethanol extraction for four days. In this preparation, 2.0 g of SBA-15 was added to the 60 ml of dry toluene containing 3 ml of EDTA, and the mixture was refluxed for 20 h. The solid product was isolated by filtration and washed with toluene, acetone and ethanol. Nickel ions were adsorbed on the surface of the EDTA grafted SBA-15. 1.2 g of functionalized silicas were mixed with 400 ml of a 10 mmol/l nickel nitrate solution ($Ni(NO_3)_2 \cdot 6H_2O$, Aldrich Chemical Co.), and it was stirred for 24 h. The pH of the solution was maintained at 5.0 to prevent the precipitation of nickel hydroxide. After filtering and drying, the sample was calcined at 673 K for 5 h to give the Ni-E-SBA catalyst.

Two types of catalyst were prepared for the comparative test. Ni-WI-SBA and Ni-WI-JRC were prepared by the wet impregnation method using SBA-15 and commercial JRC-SIO-7 (Catalysis Society of Japan) as a support, respectively. In each preparation, the support material was impregnated with appropriate amounts of aqueous nickel nitrate solution to adjust its nickel loading to 8 wt%. After successive drying at room temperature and 353 K, these catalysts were also calcined at 673 K for 5 h.

2.2. Characterization

Elemental analysis was carried out using a RECO CHNS (model 923) to confirm the EDTA grafting on the SBA-15. Nickel loading was measured using inductively coupled plasma-atomic emission spectrometry (ICP-AES; Shimazu ICPS-1000IV). N_2 adsorption/desorption isotherms were measured at 77 K using a Micromeritics ASAP 2010 sorptometer by static methods. Small-angle X-ray scattering (SAXS) patterns were collected on a Bruker GADDS diffractometer using Cu K_α radiation with 40.0 kV and 45.0 mA. Transmission electron microscopy (TEM) and transmission electron diffraction (TED) images were obtained on a JEOL JEM-2000EXII operated at 200 kV. X-ray diffraction (XRD) patterns were obtained on a MAC science M18XHF-SRA diffractometer using Cu K_α radiation with 150.0 kV and 100.0 mA.

2.3. Catalytic performances

The hydrodechlorination reaction of the prepared catalysts was investigated using 1,1,2-trichloroethane as a model compound. Experiments were performed at atmospheric pressure in a flow system equipped with a temperature-controlled furnace and a quartz reactor. The temperature was measured using a thermocouple inserted in the reactor. Liquid TCEa was fed into the reactor by a micro-feeder at a rate of 0.30 ml/h and pre-heated to 443 K before entering the reactor. Helium was used as a carrier gas at a constant flow rate of 20 ml/min and the hydrogen flow rate was 7 ml/min. The calcined catalysts were reduced before use by a hydrogen gas flow at 673 K for 2 h. Hydrodechlorination reaction was carried out at 573 K. Reaction products were sampled at the outlet of the reactor and analyzed by GC (DS 6200 FID, Donam Co.). GC/MS (GC/MSD 5973, Hewlett-Packard Co.) was used to identify the products.

3. Results and discussion

3.1. Nickel incorporation on the mesopore

ICP-AES was used to measure the nickel content of each catalyst. The amounts of nickel loaded on the Ni-E-SBA, Ni-WI-SBA and Ni-WI-JRC were 7.77, 9.42 and 8.36 wt% respectively. Diaz *et al.* [12] synthesized EDTA grafted MCM-41 (M41EDT), which was the most effective sample for the cobalt adsorption; its loading was only 3.84 wt%. Considering the fact that cobalt and nickel have similar atomic weights, this was markedly lower than that of the Ni-E-SBA. Since EDTA is a bulky organic with many carbon chains and SBA-15 has larger pore diameter than MCM-41, it is likely that more EDTA was grafted on SBA-15. This assumption is in good agreement with the elemental analysis results. The nitrogen content of the M41EDT samples was reported as 1.52 wt%, but that of EDTA-grafted SBA-15 was 2.10 wt%. In addition, the nickel loading of Ni-E-SBA was much larger than the metal loading of the catalysts prepared by ion exchange. Yonemitsu *et al.* [10] synthesized Mn-MCM-41 using the template ion-exchange (TIE) method and the manganese contents of resulting samples were less than 1.4 wt%. In the syntheses of Mn-MCM-41 and Ni-E-SBA, metal ions were incorporated on the supports by ionic interaction. However, the approach used here showed a higher metal-loading capacity with fine metal dispersion than samples prepared by ion exchange, and moreover, it was possible to adjust metal loading by changing the concentrations of the nickel ion solution at the adsorption step.

The XRD patterns for the SBA-15, Ni-E-SBA, Ni-WI-SBA and Ni-WI-JRC samples were obtained and are shown in figure 1. Regardless of the type of support used, all samples exhibited a broad silica peak around 23°, indicative of a low overall degree of crystallization of the silica supports. The XRD patterns of Ni-WI-SBA and NI-WI-JRC exhibited similar diffraction peaks at 37, 43, 62, 72 and 79°, which were characteristic of NiO(101), NiO(012), NiO(110),

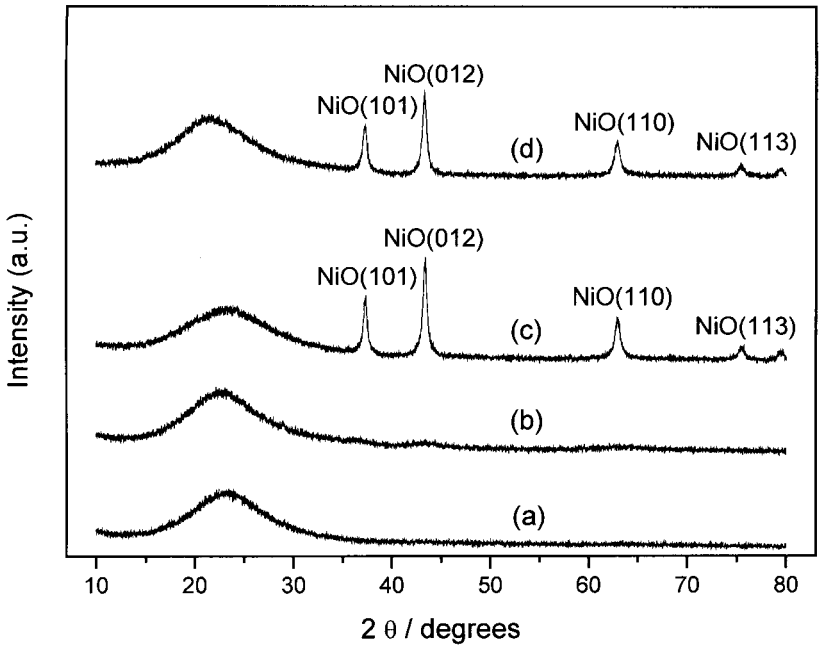

Figure 1. XRD patterns of (a) SBA-15 and the prepared catalysts after the calcination step, (b) Ni-E-SBA, (c) Ni-WI-SBA and (d) Ni-WI-JRC.

NiO(113) and NiO(202), respectively. This suggests that the crystalline structure of the nickel in the Ni-WI-SBA and Ni-WI-JRC samples was rhombohedral NiO. While crystalline phases were observed in the catalysts prepared by wet impregnation, the XRD patterns of Ni-E-SBA exhibited no recognizable specific diffraction peak of nickel species. It was similar to that of SBA-15, which was used as a support. These results suggest that the nickel was so finely incorporated on the surface of the mesopore of the Ni-E-SBA that it could not form a crystalline structure. Yuan *et al.* [18] investigated the dispersion of gold particles on titanium hydroxide and titanium oxide, using TEM and XRD. They concluded that gold particles less than 3 nm in size did not give an Au(200) peak by XRD analysis. It might be concluded that the nickel particles in the Ni-E-SBA catalyst are dispersed in nanometer size, as indicated by the XRD patterns.

Further evidence of fine nickel particle dispersion was provided by the TEM and TED images, which are presented in figures 2 and 3. SBA-15 had the regular hexagonal array of uniform two-dimensional channels, which has also been confirmed by other researchers [4]. The shape and size of the Ni-E-SBA and Ni-WI-SBA catalysts was similar to that of SBA-15 used as a support. No nickel particles were observed in the TEM images of the Ni-E-SBA catalyst, while apparent nickel particle aggregates were observed on the Ni-WI-SBA. Choi and Lee [17] synthesized nickel-loaded silica catalysts by the impregnation method and showed that the average diameter of the nickel particles in the catalysts varied from 25.2 nm to 50.6 nm. The nickel particle sizes of the samples prepared by the wet impregnation method in this work were similar to those of Choi and Lee, and the size of these particles is larger than the average pore diameter of the SBA-15, which is 8.0 nm. Therefore, it might be inferred that nickel particles formed by the wet impregnation method were loaded on the outer surface of SBA-15. In order to investigate the metal structure, TED measurement was carried out (figure 3). The TED image of SBA-15 exhibited no apparent patterns, because it did not contain metal contents. While TED images of the Ni-WI-SBA catalyst showed irregular ring patterns, weak regular hexagonal patterns were observed for the Ni-E-SBA catalyst. Nickel might be incorporated along the regular hexagonal mesopores in Ni-E-SBA. These results are consistent with nickel particles being finely dispersed along the internal mesopore surfaces of the Ni-E-SBA catalyst.

3.2. Conservation of pore structure

Figure 4 shows N_2 adsorption/desorption isotherms of SBA-15, EDTA-grafted SBA-15 and calcined Ni-E-SBA. All samples exhibited irreversible type IV adsorption isotherms with an H1 hysteresis loop as defined by IUPAC [19]. The surface area, pore diameter and pore volume of the SBA-15 decreased upon the EDTA grafting. These pore properties were, however, restored up to 64.2% (surface area) and 70.6% (pore volume) of the original value as a result of calcination in the case of the Ni-E-SBA catalyst. The hexagonal mesopore structure of the SBA-15 was not altered by the preparation procedure. The conservation of the mesoporous structure was also confirmed more precisely by the SAXS patterns, which are shown in figure 5. SBA-15 showed clear (100), (110) and (200) reflections in its SAXS diffraction

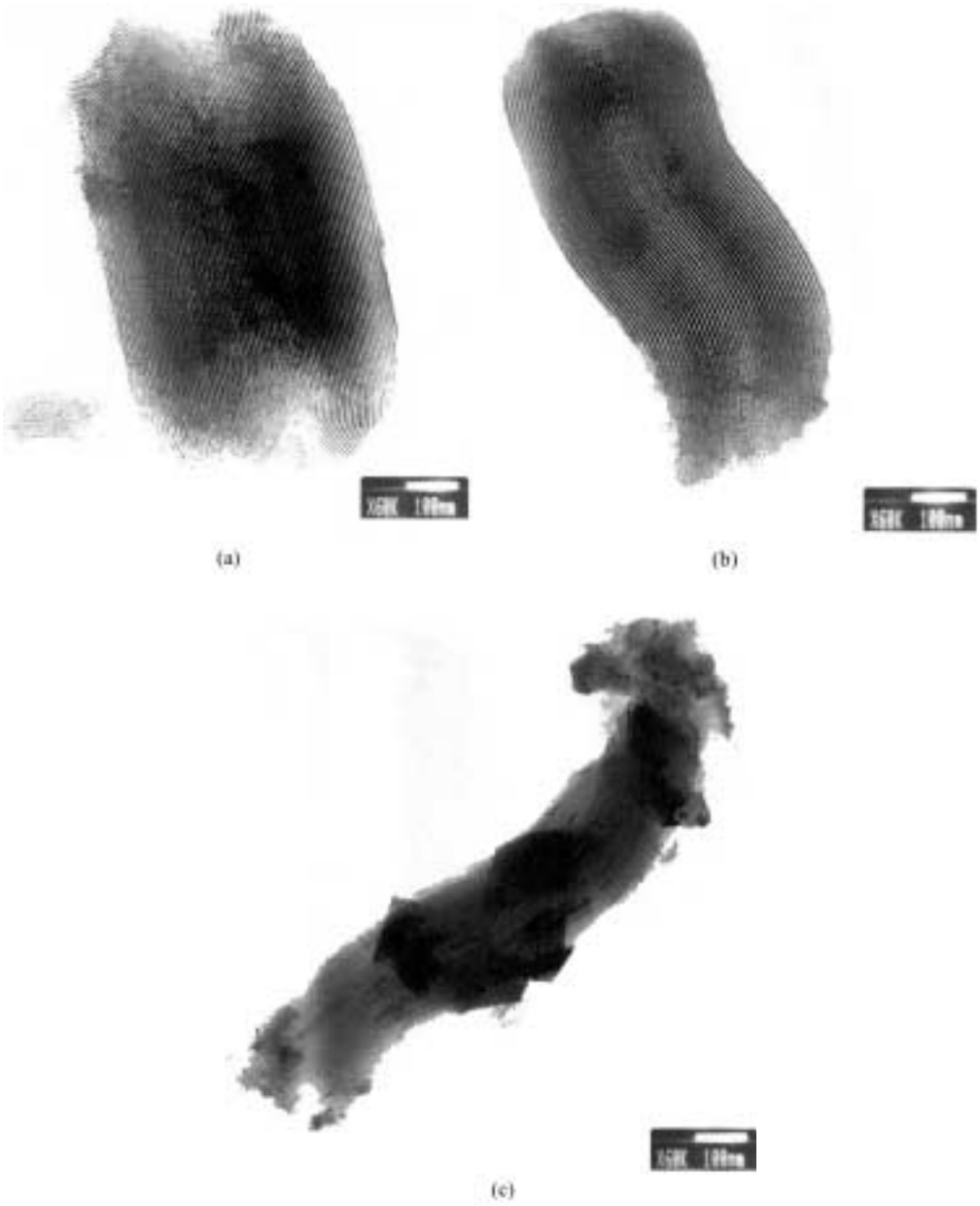

Figure 2. TEM images of (a) SBA-15 and the prepared catalysts, (b) Ni-E-SBA and (c) Ni-WI-SBA.

patterns and the 2θ angles of each peak were 0.86, 1.49 and 1.72, which suggests that SBA-15 had hexagonal mesopore structure. The peak intensity of EDTA-grafted SBA was lower than that of SBA-15 and a small decrease in the 2θ angle of the primary peak was observed. The Ni-E-SBA catalyst displayed a similar peak intensity and 2θ angles of (100) peak; however, (110) and (200) reflection was lower than those of SBA-15, which suggests that it has a lower long-range order than the original support. SBA-15 and Ni-E-SBA samples had the same primary peak at 0.86°, which indicates that the prepared materials have identical cell parameters of 11.86 nm. The comparison of the peak intensities and 2θ angles of peaks suggests that pore structure of the SBA-15 was affected by the EDTA grafting step, but original mesopore structure was restored after the calcination step. From N_2 adsorption/desorption isotherms, SAXS patterns and TEM images, it is concluded that the overall silica mesopore structure was conserved. In addition, the surface area and pore volume of the Ni-WI-SBA catalyst were decreased, because the nickel particles blocked the mesopores during the preparation steps, as shown by table 1 and figure 2(c). Consequently, Ni-WI-SBA had smaller surface area and pore volume than Ni-E-SBA. We suggest better mesopore conservation of catalysts prepared by our approach than that of catalysts prepared by the impregnation method.

3.3. *Hydrodechlorination of 1,1,2-trichloroethane*

Catalytic hydrodechlorination performances of the prepared catalysts are shown in figure 6. The Ni-E-SBA

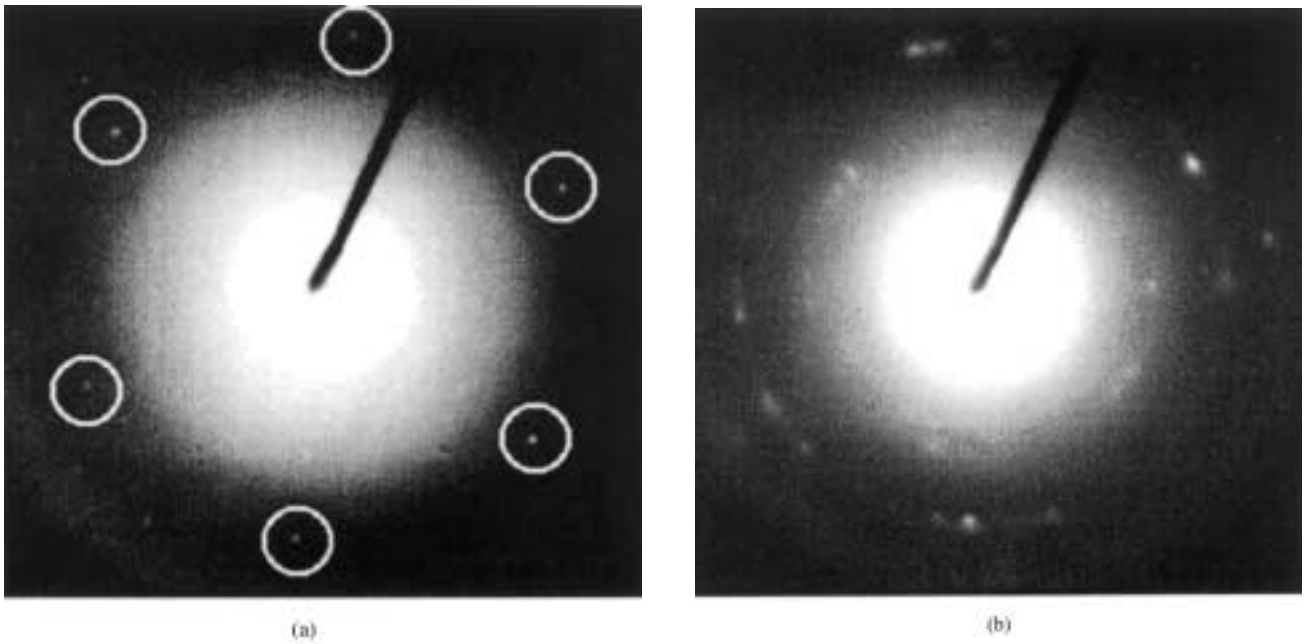

Figure 3. TED images of (a) Ni-E-SBA and (b) Ni-WI-SBA.

catalyst exhibited the highest conversion after operation of 150 min and showed the lowest deactivation of all the other catalysts examined. Choi and Lee [17] reported that Ni/SiO_2 catalysts prepared by incipient wetness impregnation could be used for the hydrodechlorination of 1,2-dichloropropane. The conversion of 10% Ni/SiO_2 catalyst, under similar reaction conditions to this study, was decreased from the initial 90% to approximately 60% during the reaction time of 20 h and thereafter remained constant. However, Ni-E-SBA catalyst with 7.77% of nickel loading showed a higher conversion of 1,1,2-trichloroethane than the conventional catalyst prepared by incipient wetness impregnation. Experimental results in figure 6 showed that a conversion of over 90% was maintained during the reaction time of 3 h and the rate of decrease is relatively small. Choi and Lee [17] reported that the nickel hydrosilicate phase was formed in nickel silica catalysts by metal–support interactions and this nickel hydrosilicate contributed to slow deactivation. Based on this observation, it is suggested that the finely dispersed nickel species show a stronger metal–support interaction and lead to nickel hydrosilicate formation and, thus, result in a higher resistance to deactivation. It should be noted that HCl is the stoichiometric product

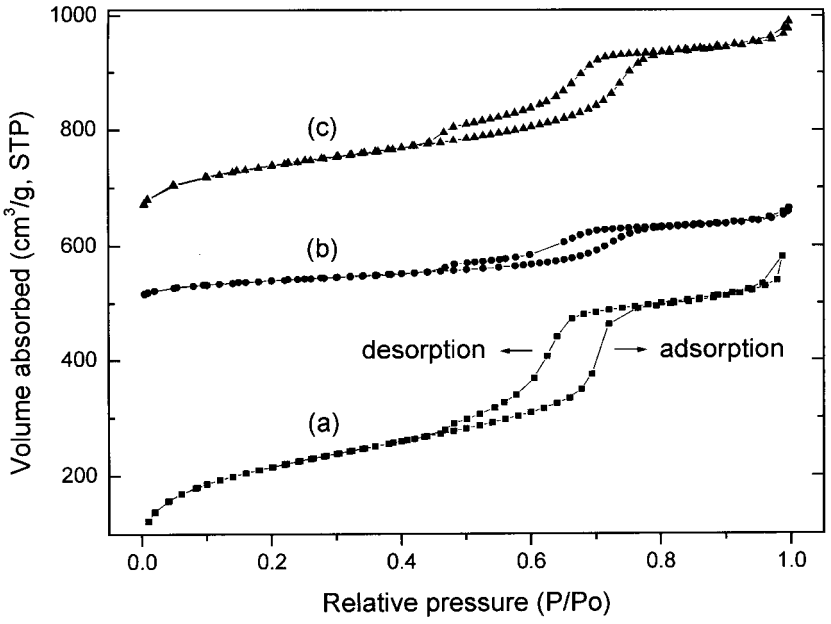

Figure 4. N_2 adsorption and desorption isotherm plots for (a) SBA-15 (■), (b) EDTA-grafted SBA-15 (●) and (c) Ni-E-SBA (▲).

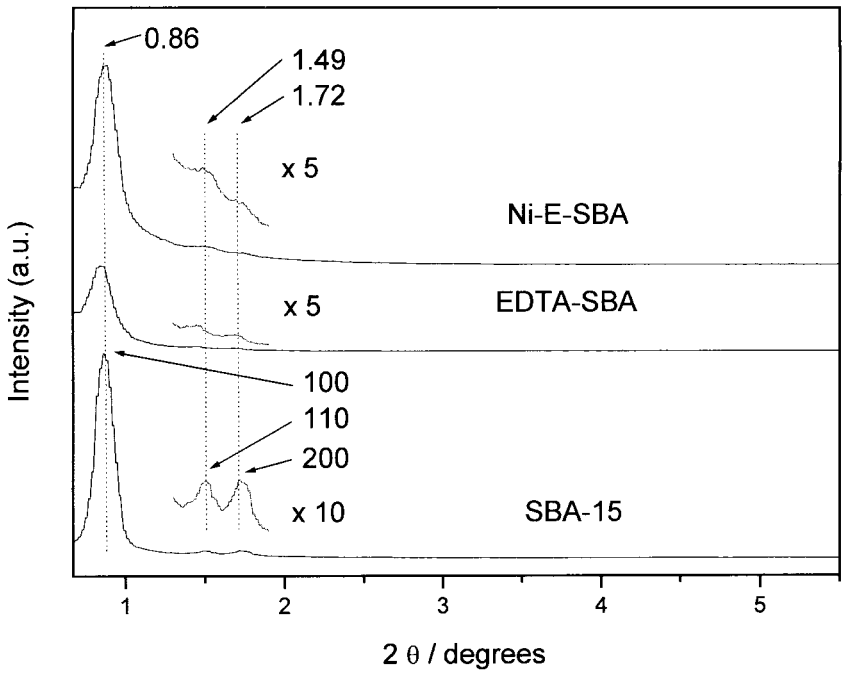

Figure 5. SAXS patterns of SBA-15, EDTA-grafted SBA-15 and Ni-E-SBA.

Table 1
Characteristics of SBA-15 and the prepared catalysts

Sample	Nickel content (wt%)	BET surface area (m^2/g)	BJH adsorption pore volume (cm^3/g)
SBA-15	0.00	783.2	0.841
Ni-E-SBA	7.77	477.0	0.493
Ni-WI-SBA	9.42	475.7	0.441
Ni-WI-JRC	8.36	184.3	0.281

of the hydrodechlorination reactions and the chlorine atoms from the reactants are known to adsorb on the nickel particles. These adsorbed chlorine atoms might reduce the metallic surface area of the catalyst and also change the oxidation state of the metal. However, the adsorbed chlorine atoms could be desorbed from the active sites as a form of HCl during the gas-phase hydrodechlorination reactions. It was observed that initially the conversion was slightly decreased and after that remained constant for several hours.

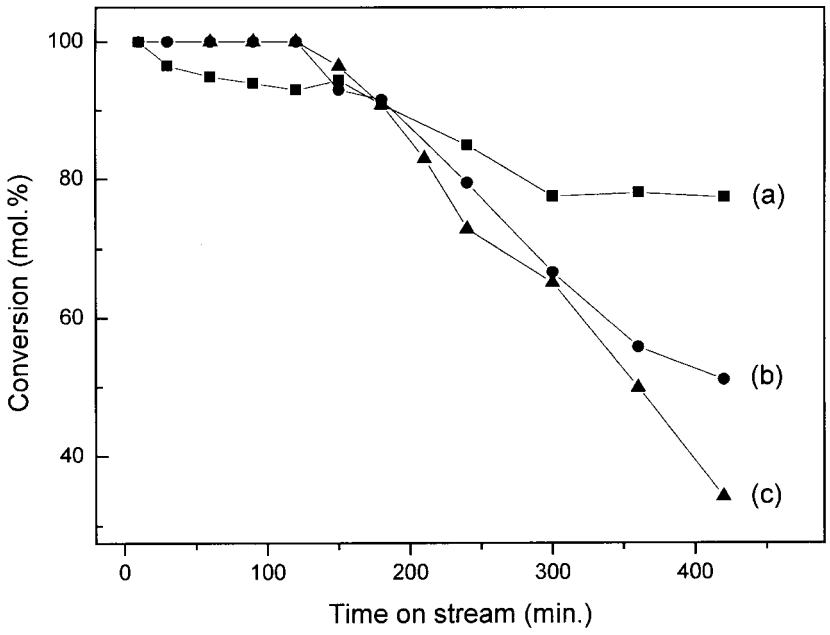

Figure 6. Catalytic activity of the prepared catalysts with respect to time-on-stream at 573 K: (a) Ni-E-SBA (■), (b) Ni-WI-SBA (●) and (c) Ni-WI-JRC (▲).

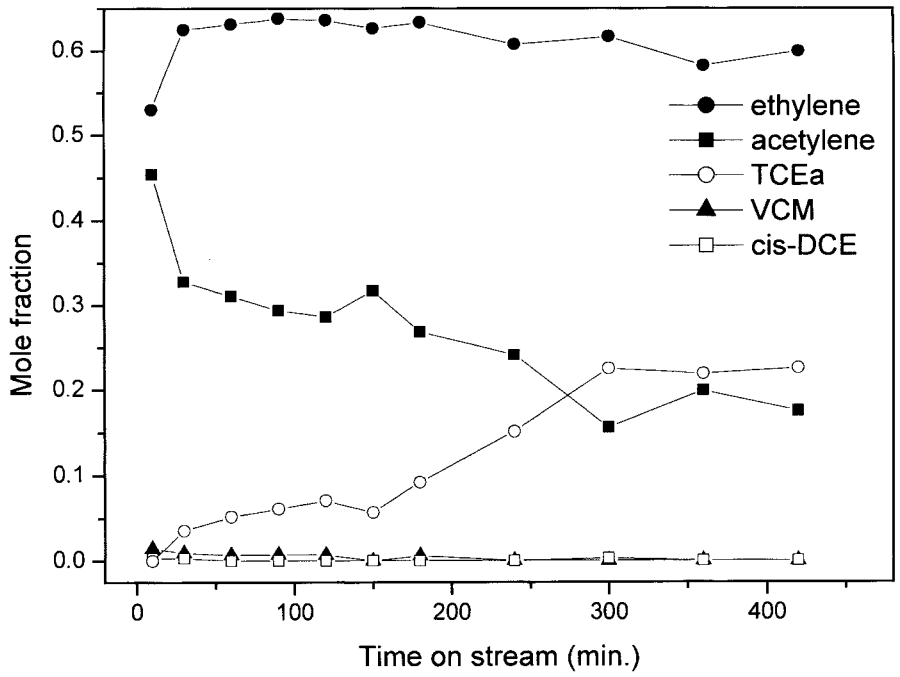

Figure 7. Product distribution of the Ni-E-SBA catalyst with respect to time-on-stream at 573 K.

Product distributions of the Ni-E-SBA catalyst are shown in figure 7. No remarkable differences in product compositions with catalysts used were observed and the major products obtained were ethylene, acetylene, vinyl chloride monomer (VCM) and cis-dichloroethene (cis-DCE). Ethylene was the major portion of the products during the reaction and acetylene was the next; however, the acetylene fraction was more affected by the catalyst activity.

The conversion by the reaction using the Ni-WI-SBA catalyst was somewhat higher than that using the Ni-WI-JRC catalyst due to its higher nickel content. We conclude that the Ni-E-SBA catalyst had more nickel hydrosilicate phase, by the fine dispersion of nickel, than those catalysts prepared by the wet impregnation methods and it leads to the lowest deactivation and the highest activity of the Ni-E-SBA catalyst among other catalysts prepared under the given conditions.

4. Conclusions

The Ni-E-SBA catalyst was synthesized using EDTA grafting, metal ion adsorption and calcinations. Using these methods, the nickel particles were finely dispersed along the surface of the mesopores of the SBA-15. The ordered mesoporous structure of the support was conserved throughout the preparation procedures. The Ni-E-SBA had high metal loading capacity. In addition, it had more dispersed metal incorporation on the mesopore than samples prepared by the wet impregnation method. The Ni-E-SBA catalyst showed the highest TCEa conversion of all the catalysts prepared in this work, and it was resistant to the deactivation in the dechlorination reaction. Further study will be needed to investigate the state of nickel particles and their size in the Ni-E-SBA catalyst and the kinetic mechanism of hydrodechlorination of TCEa over the Ni-E-SBA catalyst.

Acknowledgments

We appreciate financial aid for this research from the BK 21 Program supported by the Ministry of Education. Also, we are grateful to Ms. Mi Jung Kang of the National Center for Inter-University Facilities for the TEM and TED characterization.

References

[1] J.S. Beck, J.C. Vartuli, W.J. Roth, M.E. Leonowicz, C.T. Kresge, K.D. Schmitt, C.T-W. Chu, D.H. Olson, E.W. Sheppard, S.B. McCullen, J.B. Higgins and J.F. Schlenker, J. Am. Chem. Soc. 114 (1992) 10834; C.T. Kresge, M.E. Leonowicz, W.J. Roth, J.C. Vartuli and J.S. Beck, Nature 359 (1992) 710.

[2] T. Yanagisawa, T. Shimizu, K. Kuroda and C. Kato, Bull. Chem. Soc. Japan 63 (1990) 988.

[3] R.T. Tanev and T.J. Pinnavaia, Science 267 (1995) 865.

[4] D. Zhao, Q. Huo, J. Feng, B.F. Chmelka and G.D. Stucky, J. Am. Chem. Soc. 120 (1998) 6024; D. Zhao, J. Feng, Q. Huo, N. Melosh, G.H. Fredrickson, B.F. Chmelka and G.D. Stucky, Science 279 (1998) 548.

[5] R. Ryoo, J.M. Kim, C.H. Ko and C.H. Shin, J. Phys. Chem. 100 (1996) 17718.

[6] Z. Fu, J. Chen, D. Yin, D. Yin, L. Zhang and Y. Zhang, Catal. Lett. 66 (2000) 105.

[7] S.J. Bae, S.-W. Kim, T. Hyeon and B.M. Kim, Chem. Commun. (2000) 31.

[8] S. Jun and R. Ryoo, J. Catal. 195 (2000) 237.
[9] J.X. Zhen, S.Y. Hua and C.S. Hua, Catal. Lett. 69 (2000) 153.
[10] M. Yonemitsu, Y. Tanaka and M. Iwamoto, J. Catal. 178 (1998) 207.
[11] X. Feng, G.E. Fryxell, L.-Q. Wang, A.Y. Kim, J. Liu and K.M. Kemner, Science 276 (1997) 92; J. Liu, X. Feng, G.E. Frysell, L.-Q. Wang, A.T. Kim and M. Gong, Adv. Mater. 10 (1998) 161.
[12] J.F. Diaz, K.J. Balkus Jr., F. Bedioui, V. Kurshev and L. Kevan, Chem. Mater. 9 (1997) 61.
[13] A.M. Liu, K. Hidajat, S. Kawi and D.Y. Zhao, Chem. Commun. (2000) 1145.
[14] L. Mercier and T.J. Pinnavaia, Environ. Sci. Technol. 32 (1998) 2749.
[15] Y. Cesteros, P. Salagre, F. Medina and J.E. Sueiras, Appl. Catal. B 22 (1999) 135.
[16] G. Tavoularis and M.A. Keane, J. Molec. Catal. A 142 (1999) 187.
[17] Y.H. Choi and W.Y. Lee, Catal. Lett. 67 (2000) 155.
[18] Y. Yuan, K. Asakura, A.P. Kozlova, H. Wan, K. Tsai and Y. Iwasawa, Catal. Today 44 (1998) 333.
[19] K.S.W. Sing, D.G. Everett, W.A.W. Haul, L. Moscow, R.A. Pierotti, J. Rouquerol and T. Siemieniewska, Pure Appl. Chem. 57 (1985) 603.